

# Label-free multi-photon imaging using a compact femtosecond fiber laser mode-locked by carbon nanotube saturable absorber

K. Kieu,\* S. Mehravar, R. Gowda, R. A. Norwood, and N. Peyghambarian

College of Optical Sciences, University of Arizona, Tucson, AZ 85721, USA

\*kkieu@optics.arizona.edu

**Abstract:** We demonstrate label-free multi-photon imaging of biological samples using a compact Er<sup>3+</sup>-doped femtosecond fiber laser mode-locked by a single-walled carbon nanotube (CNT). These compact and low cost lasers have been developed by various groups but they have not been exploited for multiphoton microscopy. Here, it is shown that various multiphoton imaging modalities (e.g. second harmonic generation (SHG), third harmonic generation (THG), two-photon excitation fluorescence (TPEF), and three-photon excitation fluorescence (3PEF)) can be effectively performed on various biological samples using a compact handheld CNT mode-locked femtosecond fiber laser operating in the telecommunication window near 1560nm. We also show for the first time that chlorophyll fluorescence in plant leaves and diatoms can be observed using 1560nm laser excitation via three-photon absorption.

©2013 Optical Society of America

**OCIS codes:** (170.5810) Scanning microscopy; (180.6900) Three-dimensional microscopy; (140.7090) Ultrafast lasers; (190.4180) Multiphoton processes.

## References and links

1. W. Denk, J. H. Strickler, and W. W. Webb, "Two-photon laser scanning fluorescence microscopy," *Science* **248**(4951), 73–76 (1990).
2. K. König, "Multiphoton microscopy in life sciences," *J. Microsc.* **200**(2), 83–104 (2000).
3. W. R. Zipfel, R. M. Williams, and W. W. Webb, "Nonlinear magic: Multiphoton microscopy in the biosciences," *Nat. Biotechnol.* **21**(11), 1369–1377 (2003).
4. F. Helmchen and W. Denk, "Deep tissue two-photon microscopy," *Nat. Methods* **2**(12), 932–940 (2005).
5. E. E. Hoover and J. A. Squier, "Advances in multiphoton microscopy technology," *Nat. Photonics* **7**(2), 93–101 (2013).
6. A. C. Millard, P. W. Wiseman, D. N. Fittinghoff, K. R. Wilson, J. A. Squier, and M. Müller, "Third-harmonic generation microscopy by use of a compact, femtosecond fiber laser source," *Appl. Opt.* **38**(36), 7393–7397 (1999).
7. F. W. Wise, "Femtosecond fiber lasers based on dissipative processes for nonlinear microscopy," *IEEE J. Sel. Top. Quantum Electron.* **18**, 1412–1421 (2012.) doi: 10.1109/JSTQE.2011.2179919.
8. S. Tang, J. Liu, T. B. Krasieva, Z. Chen, B. J. Tromberg, "Developing compact multiphoton systems using femtosecond fiber lasers," *J. Biomed. Opt.* 0001;14 (3):030508–030508–3. doi: 10.1117/1.3153842.
9. G. Liu, K. Kieu, F. W. Wise, and Z. Chen, "Multiphoton microscopy system with a compact fiber-based femtosecond-pulse laser and handheld probe," *J Biophotonics* **4**(1-2), 34–39 (2011).
10. J. R. Unruh, E. S. Price, R. G. Molla, L. Stehno-Bittel, C. K. Johnson, and R. Hui, "Two-photon microscopy with wavelength switchable fiber laser excitation," *Opt. Express* **14**(21), 9825–9831 (2006).
11. K. Wang, T.-M. Liu, J. Wu, N. G. Horton, C. P. Lin, and C. Xu, "Three-color femtosecond source for simultaneous excitation of three fluorescent proteins in two-photon fluorescence microscopy," *Biomed. Opt. Express* **3**(9), 1972–1977 (2012).
12. A. V. Shubin, I. A. Bufetov, M. A. Melkumov, S. V. Firstov, O. I. Medvedkov, V. F. Khopin, A. N. Guryanov, and E. M. Dianov, "Bismuth-doped silica-based fiber lasers operating between 1389 and 1538 nm with output power of up to 22 W," *Opt. Lett.* **37**(13), 2589–2591 (2012).
13. G. Androz, M. Bernier, D. Faucher, and R. Vallée, "2.3 W single transverse mode thulium-doped ZBLAN fiber laser at 1480 nm," *Opt. Express* **16**(20), 16019–16031 (2008).
14. S. D. Jackson, "Single-transverse-mode 2.5-W holmium-doped fluoride fiber laser operating at 2.86 microm," *Opt. Lett.* **29**(4), 334–336 (2004).

15. K. Murari, Y. Zhang, S. Li, Y. Chen, M. J. Li, and X. Li, "Compensation-free, all-fiber-optic, two-photon endomicroscopy at 1.55  $\mu\text{m}$ ," *Opt. Lett.* **36**(7), 1299–1301 (2011).
16. S. Yazdanfar, C. Joo, C. Zhan, M. Y. Berezin, W. J. Akers, and S. Achilefu, "Multiphoton microscopy with near infrared contrast agents," *J. Biomed. Opt.* **15**(3), 030505 (2010).
17. M. E. Fermann, "Passive mode locking by using nonlinear polarization evolution in a polarization-maintaining erbium-doped fiber," *Opt. Lett.* **18**(11), 894 (1993).
18. K. Tamura, E. P. Ippen, and H. A. Haus, "Pulse dynamics in stretched-pulse fiber lasers," *Appl. Phys. Lett.* **67**(2), 158 (1995).
19. M. Guina, N. Xiang, and O. G. Okhotnikov, "Stretched-pulse fiber lasers based on semiconductor saturable absorber mirrors," *Appl. Phys. B* **74**(9), S193–S200 (2002).
20. T. Hasan, Z. Sun, F. Wang, F. Bonaccorso, P. Tan, A. G. Rozhin, and A. C. Ferrari, "Nanotube-polymer composites for ultrafast photonics," *Adv. Mater.* **21**(38), 3874–3899 (2009).
21. S. Yamashita, "A tutorial on nonlinear photonic applications of carbon nanotube and graphene," *J. Lightwave Technol.* **30**(4), 427–447 (2012).
22. K. Kieu and M. Mansuripur, "Femtosecond laser pulse generation with a fiber taper embedded in carbon nanotube/polymer composite," *Opt. Lett.* **32**(15), 2242–2244 (2007).
23. K. Kieu, J. Jones, and N. Peyghambarian, "Generation of few-cycle pulses from an amplified carbon nanotube mode-locked fiber laser system," *IEEE Photon. Technol. Lett.* **22**(20), 1521–1523 (2010).
24. T. H. Wu, K. Kieu, N. Peyghambarian, and R. J. Jones, "Low noise erbium fiber fs frequency comb based on a tapered-fiber carbon nanotube design," *Opt. Express* **19**(6), 5313–5318 (2011).
25. K. Kieu, A. Evans, J. Klein, J. Barton, and N. Peyghambarian, "Ultrahigh resolution all-reflective OCT system with a compact fiber-based supercontinuum source," *J. Biomed. Opt.* **16**, 106004 (2011), doi:10.1117/1.3633340.
26. R. Aviles-Espinosa, S. I. Santos, A. Brodschelm, W. G. Kaenders, C. Alonso-Ortega, D. Artigas, and P. Loza-Alvarez, "Third-harmonic generation for the study of *Caenorhabditis elegans* embryogenesis," *J. Biomed. Opt.* **15**(4), 046020 (2010).
27. D. Yelin and Y. Silberberg, "Laser scanning third-harmonic-generation microscopy in biology," *Opt. Express* **5**(8), 169–175 (1999).
28. G. O. Clay, A. C. Millard, C. B. Schaffer, J. Aus-der-Au, P. S. Tsai, J. A. Squier, and D. Kleinfeld, "Spectroscopy of third harmonic generation: Evidence for resonances in model compounds and ligated hemoglobin," *J. Opt. Soc. Am. B* **23**(5), 932–950 (2006).
29. M. J. Farrar, F. W. Wise, J. R. Fetcho, and C. B. Schaffer, "In vivo imaging of myelin in the vertebrate central nervous system using third harmonic generation microscopy," *Biophysical Journal* **100**, 1362–1371, (2011) ISSN 0006–3495, 10.1016/j.bpj.2011.01.031.
30. J.-X. Cheng and X. S. Xie, "Coherent anti-Stokes Raman scattering microscopy: instrumentation, theory and applications," *J. Phys. Chem. B* **108**(3), 827–840 (2004).
31. C. W. Freudiger, W. Min, B. G. Saar, S. Lu, G. R. Holtom, C. He, J. C. Tsai, J. X. Kang, and X. S. Xie, "Label-free biomedical imaging with high sensitivity by stimulated Raman scattering microscopy," *Science* **322**(5909), 1857–1861 (2008).
32. K. Kieu, B. G. Saar, G. R. Holtom, F. W. Wise, and X. S. Xie, "High power all-fiber picosecond laser system for coherent Raman microscopy," *Opt. Lett.* **34**, 2051–2053 (2009).
33. M. Baumgartl, T. Gottschall, J. Abreu-Afonso, A. Diez, T. Meyer, B. Dietzek, M. Rothhardt, J. Popp, J. Limpert, and A. Tünnermann, "Alignment-free, all-spliced fiber laser source for CARS microscopy based on four-wave-mixing," *Opt. Express* **20**(19), 21010–21018 (2012).
34. S. Lefrancois, D. Fu, G. R. Holtom, L. Kong, W. J. Wadsworth, P. Schneider, R. Herda, A. Zach, X. Sunney Xie, and F. W. Wise, "Fiber four-wave mixing source for coherent anti-Stokes Raman scattering microscopy," *Opt. Lett.* **37**(10), 1652–1654 (2012).
35. G. H. Krause and E. Weis, "Chlorophyll fluorescence and photosynthesis: the basis," *Annu. Rev. Plant Physiol. Plant Mol. Biol.* **42**(1), 313–349 (1991).
36. D. Kobat, M. E. Durst, N. Nishimura, A. W. Wong, C. B. Schaffer, and C. Xu, "Deep tissue multiphoton microscopy using longer wavelength excitation," *Opt. Express* **17**(16), 13354–13364 (2009).
37. M. Balu, T. Baldacchini, J. Carter, T. B. Krasieva, R. Zadayan, and B. J. Tromberg, "Effect of excitation wavelength on penetration depth in nonlinear optical microscopy of turbid media," *J. Biomed. Opt.* **14**(1), 010508 (2009).
38. N. G. Horton, K. Wang, D. Kobat, C. G. Clark, F. W. Wise, C. B. Schaffer & C. Xu, "In vivo three-photon microscopy of subcortical structures within an intact mouse brain," Published online: 20 January 2013 | doi:10.1038/nphoton.2012.336.

## 1. Introduction

Multi-photon (MP) imaging is a powerful technique that allows three dimensional mapping of samples that have a measurable nonlinear optical response such as SHG, THG or fluorescence induced by MP absorption. This provides us with a way to see the nonlinear microscopic world with high resolution, in 3D. After about two decades of intensive development MP

imaging (MPI) has found important applications in biological research and in diagnosing medical conditions [1–5]. Among the main remaining barriers to making MPI a widespread diagnostic and research tool are the size and cost of the MP microscope; currently only major research institutions can afford to purchase, house and maintain them. We seek to address this challenge by developing more compact and affordable MPI microscope systems in order to make them available to a greater number of researchers and, ultimately, hasten their adoption in medical testing. New applications, ideas, and discoveries are certain to emerge just from the high throughput and reliability of these unique instruments. The laser source normally comprises a major part of the total cost of a typical MP microscope. So a clear approach to solve the outstanding problems mentioned above is to create new, robust and low cost ultrafast laser sources that are suitable for MPI. Ultrafast lasers based on Ti:sapphire (Ti:sa) crystals have played an important role in the early stage of MPI development. They are currently still the work-horse of the field due to their versatility and good performance. However, there is a consensus in the research and applications communities that these lasers are not currently suitable for applications outside of the research laboratory environment. Fiber lasers, on the other hand, are quite attractive owing to their compactness, freedom from alignment issues and potentially much lower cost. Recently, there has been a strong push to develop low cost fiber lasers for MPI [6–11]. Promising results have been published, but it is not yet clear if fiber lasers will be able to fully replace the standard Ti:sa laser for MPI.

There are three established wavelength ranges where fiber lasers work well owing to the existence of suitable rare-earth ions.  $\text{Er}^{3+}$ -doped fibers cover the 1550nm range (roughly 1520-1630nm),  $\text{Yb}^{3+}$ -doped fibers work in the 1020-1100nm range, and  $\text{Tm}^{3+}$ -doped fibers provide access to the 1850-2000nm region. All of these gain fibers are based on silica host glass where very low loss transmission and good fiber mechanical strength can be achieved. There are other types of fibers that have been investigated that may open up new operating windows in the visible, near-IR and mid-IR range [12–14]. The newly developed bismuth doped silica fiber [12] may be important for MPI since it provides access to the 1300nm wavelength region, where biological tissues are not too absorbing. The longer wavelengths accessible with this gain medium may help increase the MP imaging depth significantly due to the reduced scattering loss.

Ultrafast fiber lasers have been successfully used for MPI [6–11].  $\text{Yb}^{3+}$ -doped fiber lasers can be applied directly to perform TPEF, SHG and THG imaging. Frequency doubling to  $\sim 780\text{nm}$  is normally preferred for  $\text{Er}^{3+}$ -doped fiber lasers working near 1550nm since water absorption in biological tissue is often considered too high at 1550nm and beyond. In general, it is easier and lower cost to build a compact ultrafast laser based on  $\text{Er}^{3+}$ -doped fiber due to the availability of fiber components already developed for telecommunications. In addition, a large selection of fibers with different dispersion values is commercially available which facilitates the design and construction of mode-locked laser sources at this wavelength. If the 1550nm wavelength can be used directly for MPI, it could be the solution to bringing this powerful technique to more applications [15, 16]. Currently, nonlinear polarization evolution (NPE) and semiconductor saturable absorber mirrors (SESAM) are widely used to achieve mode locking in fiber lasers [17–19]. However, these two techniques have drawbacks. NPE requires additional elements in the cavity, including a polarizer and waveplates. Furthermore, fiber lasers mode-locked with NPE are generally not environmentally-stable since any change in temperature or any movement of the fiber in the cavity can change the mode-locking condition. SESAMs have become readily-available, but tend to damage in fiber lasers, perhaps owing to the large modulation depth that is needed from the thin film absorber geometry. Saturable absorbers (SA) based on carbon nanotubes (CNT) have recently attracted attention from many researchers worldwide owing to their simplicity in fabrication and low cost [20, 21]. Using this new material, we have developed a new type of SA based on a fiber taper that is embedded in a CNT/polymer composite [22]. The interaction between light and CNTs happens through the evanescent field of a fiber taper. The design of the CNT SA that

we developed is advantageous compared to other designs based on thin film format where absorption happens in a thin film of  $<1\mu\text{m}$  thickness. In our CNT SA, the absorption happens in a distributed way along a fiber taper ( $>10\text{mm}$  in length). For that reason the generated heat is distributed along a long path making our SA design very robust to thermal damage. We have previously shown that mode-locked fiber lasers based on CNT can be used in important applications such as supercontinuum generation, frequency comb metrology, and OCT imaging [23–25]. However, the capability of this new technology for MPI has not yet been investigated. We believe this new ultrafast laser platform may be the key to moving MPI into the hands of more researchers and into broader applications.

In this communication, we would like to present our latest results regarding the use of compact CNT mode-locked ultrafast  $\text{Er}^{3+}$ -doped fiber lasers for MPI of different biological samples. It is shown that various imaging modalities (e.g., SHG, THG, TPEF, and 3PEF) can be effectively performed using laser excitation at telecommunication wavelengths near 1560nm. A recent publication [26] has also shown that the expected water absorption at this wavelength did not compromise sample viability. The benefits of using ultrafast  $\text{Er}^{3+}$ -doped sources are many including the following: 1) the cost of the carbon nanotube modelocked excitation laser will be much lower (an order of magnitude below that of Ti:sa lasers); 2) longer wavelength operation may lead to larger imaging depth; 3) excitation with longer wavelengths reduces photo-toxicity of the sample; 4) THG imaging [27–29], an important label-free technique, can be implemented quite easily since the emission wavelength is in the visible where standard collection optics and photomultiplier tubes (PMT) for detection work best; 5) the laser beam can be delivered to the microscope using optical fiber, reducing the alignment effort; and, finally, 6) this is an excitation wavelength that has not been thoroughly explored for MPI, providing the opportunity for new discovery.

## 2. Multiphoton microscope and excitation laser

In general, there are two ways of getting high imaging contrast with MP excitation. The first approach is to introduce molecules with a desirable nonlinear optical response to the sample which would target certain structures or areas in the sample that need to be visualized. This approach provides a strong MP signal in targeted areas for imaging, which is why it is currently used by many research groups. The drawback is the need for specially designed, potentially toxic molecules that must be artificially introduced, resulting in either higher cost or significant sample modifications. The second approach is to rely on the inherent nonlinear optical response of the sample itself, without introducing any imaging contrast agent from outside. This label-free approach is simple and does not have the serious drawbacks described above, but it can be used to image only a limited class of samples with endogenous MP chromophores, or structures with strong SHG and/or THG response. Coherent Raman microscopy (CRM) is also a very interesting label-free MPI modality where the signal is generated from the Raman vibrations of endogenous molecules. The challenge with this technique is the need for two synchronized ultrafast laser pulse trains, still not straightforward to implement with state-of-the-art laser technology [30, 31]. Nevertheless, there have been promising reports recently on laser source development for CRM [32–34].

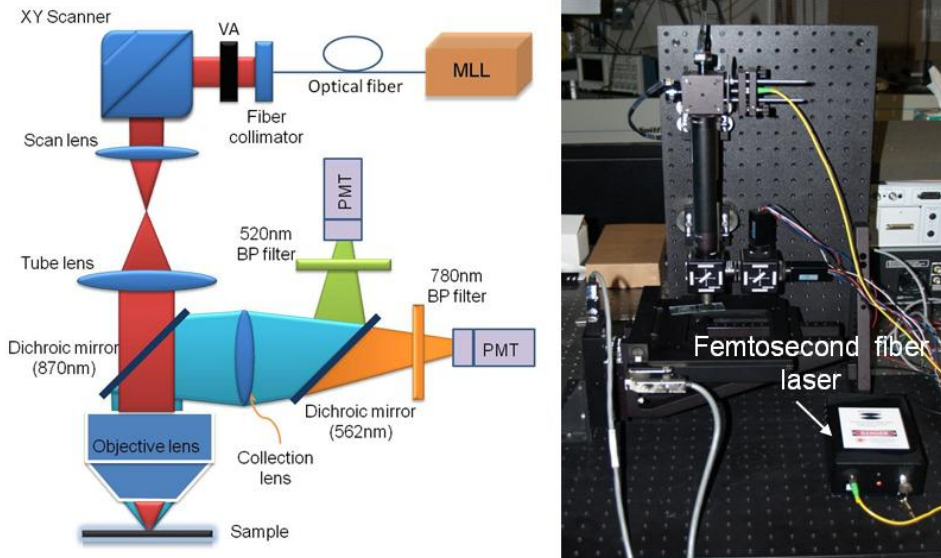


Fig. 1. Left: Schematic diagram of the multi-photon microscope. MLL: mode-locked fiber laser with carbon nanotube saturable absorber. VA: variable attenuator. Right: A photograph of the actual microscope, the handheld femtosecond fiber laser is also shown.

Many multiphoton microscopes are built around standard commercial microscopes for convenience. MPI requires excitation in the near-IR range where femtosecond sources exist. However, standard microscopes are often designed for visible wavelengths. Hence, the transmission loss for the excitation laser to the sample is normally quite high and only around 50% or less of the excitation laser typically makes it through the microscope optics to the sample surface. The problem becomes more severe when 1560nm or longer wavelengths are used for MPI, where microscope throughputs of  $\sim 1\%$  have been reported in [26]. Besides the problem with low transmission throughput, the use of wavelengths outside of the designed range may create problems with aberration and field curvature. For that reason, we designed and purpose-built the MP microscope used for this investigation. This provided the ability to select optical elements that are optimized for 1560nm wavelength operation to minimize transmission loss through the whole system as well as optical aberration. The schematic diagram of our multi-photon microscope is shown in Fig. 1 (left). The excitation laser is an all-fiber femtosecond laser based on  $\text{Er}^{3+}$ -doped gain fiber. The laser is mode-locked with a carbon nanotube saturable absorber based on a fiber-taper design as reported in [22]. The laser oscillator is amplified using a core-pumped  $\text{Er}^{3+}$ -doped amplifier to about 60mW average output power (limited by available 980nm pump power). The laser system is designed so that the pulses coming out of the output fiber's end achieve nearly their shortest duration just before entering the microscope. The design of the amplifier is similar to that reported in [23]. The whole laser system can be built with all-fiber components, avoiding the need for difficult free-space alignment. As the result, the entire system including pump laser and electronics can be packaged in a handheld box with dimensions of only  $20 \times 12 \times 5\text{cm}$  (Fig. 1). The laser output is collimated using a fiber collimator (Thorlabs, F280APC-1550), and the collimated beam is scanned in the  $xy$ -plane with a 2D galvo-scanner (Thorlabs, GVSM002). The beam is then relayed and expanded using a telescopic system formed by two achromatic doublets. The dimensions of the system are set such that the first galvo mirror is imaged onto the back aperture of the focusing objective to avoid signal variation during scanning. The objective we use for imaging is just an aspheric lens with 0.5NA which is AR coated for 1550nm wavelength (New Focus, 5723-H-C). The lateral and axial resolution achievable with the aspheric lens for THG imaging was measured to be  $\sim 1.1\mu\text{m}$  and  $7.3\mu\text{m}$ ,

respectively, using a nano-waveguide chip made of silicon as the sample (Fig. 2). The lateral resolution is better than the diffraction limited spot size ( $\sim 1.8\mu\text{m}$ ) due to the nonlinear response nature of the THG signal. We use the non-de-scanned detection scheme to detect the generated nonlinear signals. The excitation laser and the generated signals are separated using a dichroic filter with its cutoff wavelength at  $\sim 870\text{nm}$  (Semrock). A second dichroic filter with its cutoff wavelength at  $562\text{nm}$  is used to split the signal into two channels for simultaneous recording. Two identical PMTs (Hamamatsu, H10721-20) are used in the two channels for detection. The short wavelength channel is used for THG imaging where a band-pass filter at  $520\text{nm}$  (20nm pass-band, Semrock) is used before the PMT. The second channel can be used for 3PEF, TPEF or SHG imaging (depending on the band-pass filter used in front of the PMT). The signals from the PMTs are amplified using low noise current amplifiers (Stanford system, SR570) before being digitized with a PCI data acquisition card (NI, PCI-6115). The control software is ScanImage, and the sample is attached to a  $xyz$  motorized stage (ASI, LXI4000) which can be computer-controlled via a Matlab interface embedded in ScanImage.

### 3. Results and discussion

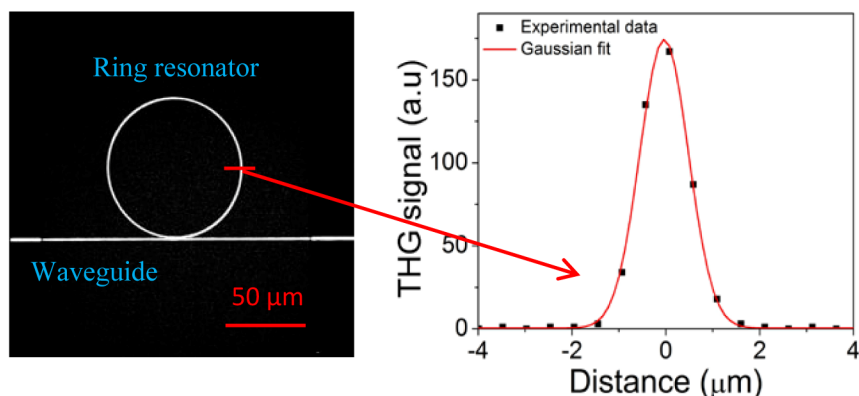


Fig. 2. : *Left*: THG image of a silicon photonic chip. We observed a strong THG signal from the nano-waveguide coupled to the ring resonator ( $200\times 100\text{nm}$ ). *Right*: THG signal profile across the ring resonator showing axial resolution of  $\sim 1.1\ \mu\text{m}$ . The frame rate was  $\sim 3\text{s}/\text{frame}$ .

Figure 3 shows an example of MPI of a fresh leaf from an indoor plant. Without any special contrast agent, we were able to detect strong THG signal from lipid cell layers within the leaf. Interestingly, we also detected 3PEF emission in the  $650\text{-}750\text{nm}$  range (Fig. 3), which we attribute to chlorophyll species, since these molecules are known to have strong fluorescence emission in this spectral range [35]. Early work [6] on the THG imaging of plant leaves with a  $1560\text{nm}$  excitation wavelength did not reveal this signal, so we believe that this is the first time that 3-photon excitation fluorescence of chlorophylls has been reported at this excitation wavelength. To explore further we have also recorded an image of a small fresh mesquite leaf. The leaf was small enough that we could record the image of the whole structure using the tiling technique (Fig. 3, right). It is apparent that the lipid cell layers (which generate the THG signal) in the mesquite leaf (mesquite is a desert plant native to Arizona) are much fewer compared to what was seen from the indoor plant. Our approach may provide a new tool for the study of photosynthesis where the chlorophyll distribution can be obtained in 3D with high resolution. The average laser power we used to acquire the image was only  $30\text{mW}$ . The pulse duration at the sample surface was  $\sim 150\text{fs}$  and the pulse repetition rate was  $50\text{MHz}$ .

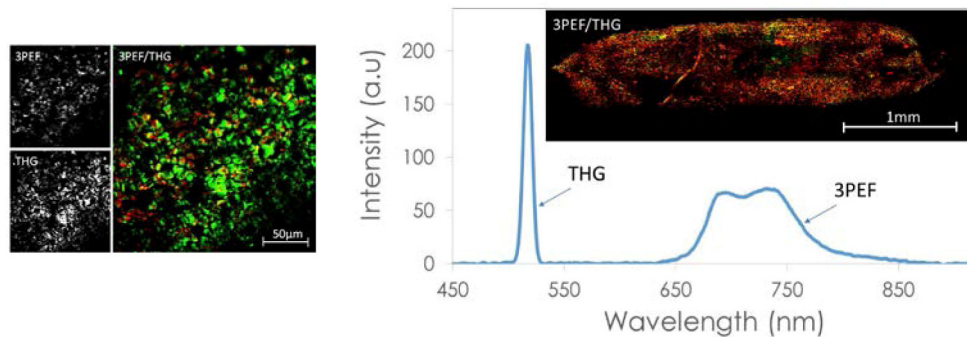


Fig. 3. *Left*: Multi-photon image of a fresh leaf from an indoor plant. We observed a strong THG signal (green) from lipid cell layers and a 3PEF signal (red) from chlorophyll. *Right*: Optical spectrum of the generated light due to the femtosecond laser excitation. Inset: Multi-photon image of a whole mesquite leaf. Mesquite is a desert tree native to Arizona. The image was composed by tiling 56 frames. The frame rate was  $\sim 3$ s/frame.

As with the fresh leaves, a strong THG signal was also produced by lipid cell layers inside the chloroplasts and 3PEF was emitted from chlorophyll of living centric diatoms *Coscinodiscus wailesii* (Fig. 4, left); we believe this to be the first time that living diatoms have been imaged with an MP microscope. Furthermore, strong multiphoton signals were also observed for the non-centric diatoms *Pyrocystis fusiformis* (Fig. 4, right). We mapped out the spatial distribution of the chloroplasts inside the diatoms with  $\sim 1\mu\text{m}$  resolution; note that the resolution can be pushed to  $\sim 0.5\mu\text{m}$  using a lens with a higher NA. This may allow us to explore the efficient photosynthesis machinery of diatoms, which is little understood. Interestingly, we can image living organisms in an underwater environment ( $\sim 200\mu\text{m}$  from the water surface) using a 1560nm femtosecond laser even though this laser wavelength has been avoided in the past due to water absorption concerns. In addition, we were able to image the centric diatoms continuously for days without damaging them with the laser radiation; clearly our exploitation of telecommunications wavelengths and lasers shows that this region is an untapped landscape for MP microscopy.

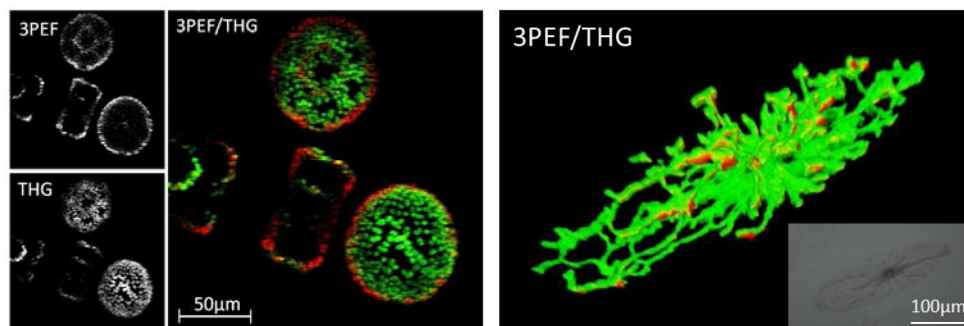


Fig. 4. *Left*: Multi-photon image of living centric diatoms *Coscinodiscus wailesii*. As with the fresh leaf, we observed strong THG signal (green) from lipid cell layers inside the chloroplasts and 3PEF signal (red) from chlorophyll. *Right*: 3D view of a 3PEF and THG image of a living non-centric diatom *Pyrocystis fusiformis*. Inset: Optical image of the non-centric *Pyrocystis fusiformis* diatom. [Media 1](#) shows the  $z$ -sections of diatoms *Coscinodiscus wailesii* recorded with our multiphoton microscope. [Media 2](#) shows the 3D rendering of the *Pyrocystis fusiformis* diatom shown on the right. The  $z$ -step size is  $1\mu\text{m}$ . The frame rate was  $\sim 3$ s/frame.

To explore further, we imaged different fixed biological samples (prepared microscope slides purchased from Amscope.com) such as mosquitos, *Drosophila*, mouse organs, etc. It turns out that most samples we have inspected have strong SHG and THG response which

can be used to perform label-free MPI. Figure 5 shows some representative images of a thin section of a mouse kidney and striated muscle tissue. Most cell structures generated THG signal whereas connective tissues provided the SHG signal. The signal to noise ratio of the acquired images was quite good with an acquisition time of less than three seconds.

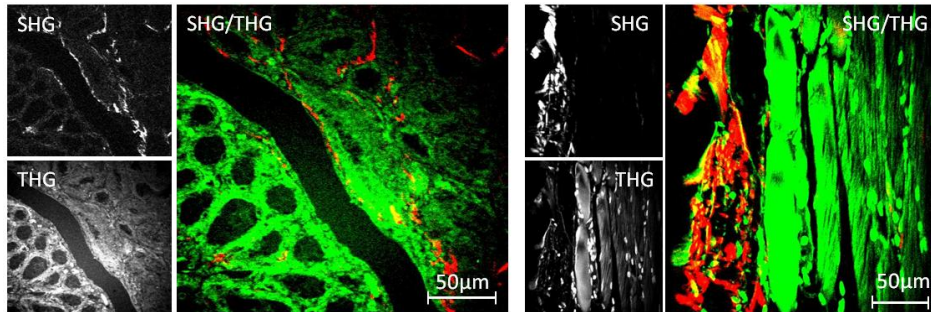


Fig. 5. SHG (red) and THG (green) image of a thin section of a mouse kidney and a thin section of striated muscle tissue. The frame rate was  $\sim 8$ s/frame

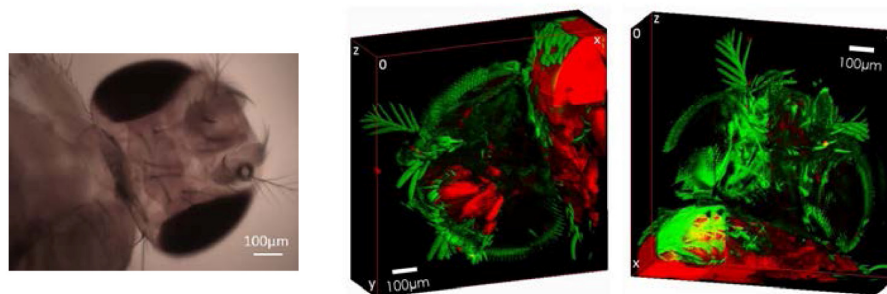


Fig. 6. *Left*: Optical image of a *Drosophila* head. *Center and Right*: 3D reconstruction of a *Drosophila* head received by tiling 20 separate stacks. We observed strong THG signal (green) as well as SHG signal (red) from different tissue structures. The SHG signal seemed to come from muscle tissues while the THG signal was generated from the other type of tissues including the outer layers which are rich in chitin. *Center*: The back view and *Right*: the front view of the head. The thickness of the head is  $220\mu\text{m}$  and the size of the head in the  $xy$ -plane is about  $1\text{mm} \times 1\text{mm}$ . [Media 3](#) shows the 3D rendering of the *Drosophila* head. The frame rate was  $\sim 3$ s/frame.

One interesting feature of using long wavelength excitation is the possibility of increasing the imaging depth in highly scattering tissue. Mouse brain tissue or model phantom samples have been used as test objects to assess and compare the imaging depth capability of different excitation lasers [36, 37]. We lack access to mouse brain samples so we used small insects and zebra-fish as the means to estimate the imaging depth that can be achieved with 1560nm femtosecond laser excitation. During the course of this investigation we found out that most insects expressed very strong THG signal (especially the outer shell layer) under interaction with a focused near-IR laser beam. It is clear that this new wavelength window is very attractive for studying the biology of small animals since it is possible to image the whole body of the animal quite easily without the need for any extraneous contrast agent. Figure 6 shows a THG image stack acquired from a *Drosophila* head fixed on a microscope slide and protected with a glass cover slip (Amscope). It was possible to image all the way through the head of the insect as can be seen in Fig. 6. The thickness of the *Drosophila* head was around  $220\mu\text{m}$ . We have also performed in-vivo imaging of a Zebra fish embryo (5 days old). There were strong THG signals from the fish's eyes and pigmentation patterns and SHG signal from the fish's muscle tissue. Figure 7 shows the 3D reconstruction and image sections recorded at different depths of the Zebra fish eye. The imaging depth here was around  $240\mu\text{m}$  as well.



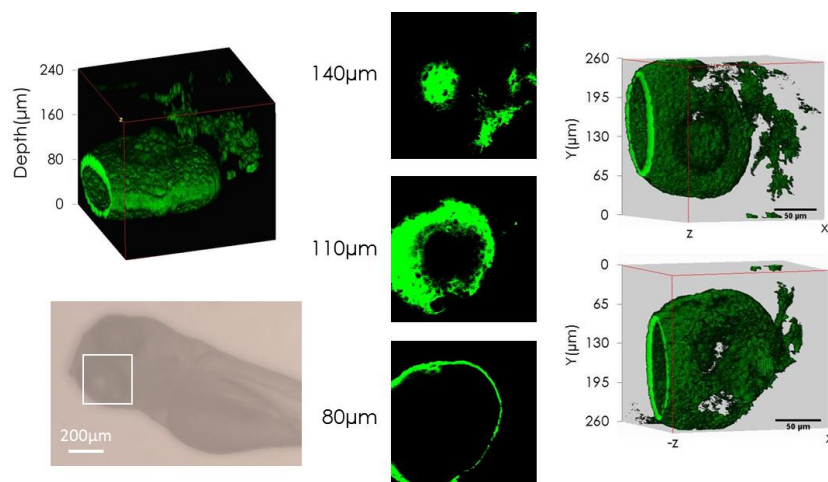


Fig. 7. *Left*: 3D reconstruction of the Zebra fish eye and standard optical image of the fish. The fish embryo was 5 days old and it was fixed in agarose gel for in-vivo imaging. *Middle*: Examples of images from different depths. *Right*: The 3D front view (*up*) and the back view (*down*) of the eye. We observed strong THG signal (green) from inside the Zebra fish eye. [Media 4](#) shows the 3D rendering of the fish eye. The frame rate was  $\sim 8$ s/frame.

## 5. Conclusions and outlook

We have demonstrated that compact mode-locked fiber lasers in the telecommunication wavelength range (around 1560nm) using CNT SA can be used directly to perform label-free multiphoton imaging of different biological samples. We have observed for the first time, to the best of our knowledge, 3PEF from chlorophyll in fresh plant leaves and living diatoms. Multiphoton excitation with longer wavelengths in the 1550-1800nm window may be important in revealing a world that is otherwise hidden when using shorter excitation wavelengths that standard Ti:sa lasers provide. The greatest advantages include low cost laser sources and deeper imaging capability due to reduced scattering loss (as has recently been demonstrated in [38]). We have shown modest imaging depth on different samples with only  $\sim 1$ nJ laser pulse energy. There is an excellent potential to improve the penetration depth further by using sources with higher pulse energy and shorter pulse duration. Moving to slightly longer wavelengths around 1650nm [38] will also provide additional advantages in imaging depth and reduce potential sample heating issue, since water absorption in this wavelength range is a few times smaller than that at 1560nm.

## Acknowledgments

Support from the CIAN NSF ERC under grant #EEC-0812072, the State of Arizona's TRIF funding and the Center for Insect Science (University of Arizona), the Air Force Office of Scientific Research BioPAINTS MURI (Award # FA9550-10-1-0555) are gratefully acknowledged. We would like to thank Prof. G. Spirou and Dr. L. Zhang from West Virginia University for providing us the interface Matlab code for controlling the *xyz* motorized stage which we modified and incorporated to ScanImage. We would like to take this opportunity to thank Dr. Vijay Iyer of Janelia Farm for providing ScanImage to the community and for his support during the construction of the microscope. Contribution from Dr. Patrick Williams to the early stage of this work is acknowledged. We would also like to thank Prof. L. Peng at the College of Optical Sciences for providing the Zebra fish embryo sample.